Generalized Skyrme model with the loosely bound potential

Sven Bjarke Gudnason,[1,*] Baiyang Zhang,[1,†] and Nana Ma[2,1,‡]

[1]*Institute of Modern Physics, Chinese Academy of Sciences, Lanzhou 730000, China*
[2]*School of Nuclear Science and Technology, Lanzhou University, Lanzhou 730000, China*

We study a generalization of the loosely bound Skyrme model which consists of the Skyrme model with a sixth-order derivative term—motivated by its fluidlike properties—and the second-order loosely bound potential—motivated by lowering the classical binding energies of higher-charged Skyrmions. We use the rational map approximation for the Skyrmion of topological charge $B = 4$, calculate the binding energy of the latter, and estimate the systematic error in using this approximation. In the parameter space that we can explore within the rational map approximation, we find classical binding energies as low as 1.8%, and once taking into account the contribution from spin-isospin quantization, we obtain binding energies as low as 5.3%. We also calculate the contribution from the sixth-order derivative term to the electric charge density and axial coupling.

I. INTRODUCTION

The Skyrme model was proposed as a toy model for baryons in a low-energy effective theory of pions [1,2]. The baryon in this theory is identified with the soliton of the theory—the Skyrmion. In the large-N_c limit of QCD, this identification is shown by Witten to be exact [3,4]. Soon after many properties of the nucleon were calculated in the framework of the (standard) Skyrme model, see, e.g., Refs. [5,6]. It took a while, however, before progress was made on higher baryon numbers, and the breakthrough came with an approximation using a rational map [7–9]. The Skyrmion is a map from point-compactified 3-space, which is topologically equal to a 3-sphere, to the isospin SU(2), which is also a 3-sphere. The rational map approximation[1] is an assumption that the 3-sphere can be factorized into a radial direction ($\mathbb{R}_+$) times a 2-sphere. The latter 2-sphere is then mapped to a 2-sphere in the target space using the rational map, being a map between Riemann spheres of degree B. The total configuration also has topological degree B, and B is identified with the baryon number. This approximation turned out to be a good approximation for a range of baryons from $B = 1$ through $B = 22$—in the case of massless pions—producing fullerenelike structures.

Turning on a physically reasonable pion mass, however, turned out to induce some alterations [10–12]; namely, the

fullerenes are no longer the global minimizers of the energy, and the Skyrmions prefer to organize them selves in a crystal made of cubic 4-Skyrmions [13]. This revelation of the 4-Skyrmion—which is also the alpha particle in the model due to unbroken isospin symmetry—playing an important role in composing nuclei, turned out to be a welcome feature in the light of nuclear clustering [14]. The identification of the cluster states in carbon-12 within the Skyrme model framework [15] is one of our main motivations for using and improving the Skyrme model.

Many properties of nuclei can be studied after this ground work has been carried out and new nuclear clusters can be studied. However, one notorious problem remains; namely, the binding energies of the multi-Skyrmions turn out to be about 1 order of magnitude too large, compared with experimental data. This has motivated a line of research trying to modify the Skyrme model so as to produce much smaller binding energies. The experimental fact that the binding energies are almost vanishing led theorists to think that a (deformed) BPS-type model would be a good candidate for reproducing the low values of the binding energies. The first direction was inspired exactly by this and started off with a selfdual Yang-Mills theory in five dimensions, yielding the Skyrme model in four dimensions with an infinite tower of vector mesons [16,17]. Another proposal came with the discovery of a BPS subsector in the Skyrme model that is saturable [18–20], unlike the Skyrme-Faddeev bound of the standard Skyrme model [1,2,21] for which no solutions saturate it in flat space [22].[2] This BPS subsector consists of the baryon current squared and a potential; thus, no standard kinetic terms are present in this theory. However, this sector is integrable, and the theory

---

*bjarke@impcas.ac.cn
†zhangbaiyang@impcas.ac.cn
‡mann13@lzu.edu.cn
[1]Throughout the paper, we will call it the rational map approximation as opposed to the misleading term rational map ansatz sometimes used in the literature. It is not an ansatz in the sense that the functions of the ansatz do not provide a solution to the field equations. It is an approximation—and a rather good one for massless pions—in that it reproduces approximate solutions with only about 1%–2% higher energy than the true solutions.

[2]A solution saturating the energy bound exists on a 3-sphere of a certain radius [22]; this is not so useful for nuclei though.

---

possesses an infinite amount of symmetries corresponding to volume-preserving diffeomorphisms. It also has the advantage of modeling a perfect fluid, which is a welcomed feature in nuclear matter and neutron stars [23–26]. It is by now called the BPS-Skyrme model. The problem of perturbing this model is that its near-BPS regime yields parametrically large field gradients that obviously are very hard to tackle in numerical calculations using the finite difference method [27,28]. Our motivation for including this term is its fluidlike properties and that it allows for a limit where the binding energies are small.

In this paper, we follow a third path, inspired by an energy bound valid for a certain potential [29], which is basically the standard Skyrme model with a repulsive potential of fourth-order in $\sigma = \text{Tr}[U]/2$,

$$V = \frac{1}{4}m_4^2(1-\sigma)^4,$$

where U is the field in the usual chiral Lagrangian [27]. This model was dubbed the lightly bound Skyrme model. Soon after a better potential was found in Ref. [30], which is of same type but only second order in σ

$$V = \frac{1}{2}m_2^2(1-\sigma)^2.$$

By better, we mean that it can produce lower binding energies for the multi-Skyrmions without breaking the platonic symmetries of the low baryon numbers; in particular, without breaking the cubic symmetry of the 4-Skyrmion responsible for clustering in the Skyrme model [30]. We call this model: the loosely bound Skyrme model and correspondingly, the potential: the loosely bound potential. In Ref. [31], we have explored the most general potential up to second order in σ and varied the value of the pion mass in order to find the optimal point in the minimal loosely bound Skyrme model. In terms of low binding energies, the model prefers a large pion mass and a large value of the coefficient of the loosely bound potential.

In order to improve the remaining issue of too-large binding energies, we will in this paper include the BPS-Skyrme term. The various regimes of the parameter space are sketched in Fig. 1.

As explained in the figure caption, in region A, the BPS-Skyrme term is relatively small and the normal Skyrme model terms are still sizable; this is the regime we will study in this paper. B is the region of parameter space where m_2 can be larger due to the presence of a medium-sized value of c_6; this is of course just our expectation and the exploration of this regime (if it exists) requires full partial differential equation (PDE) calculations. Finally, in regime C both the BPS-Skyrme term and the potential are huge such that the kinetic term and the normal Skyrme term are mere perturbations of the BPS-Skyrme model. This regime is highly nontrivial due to technical problems in the
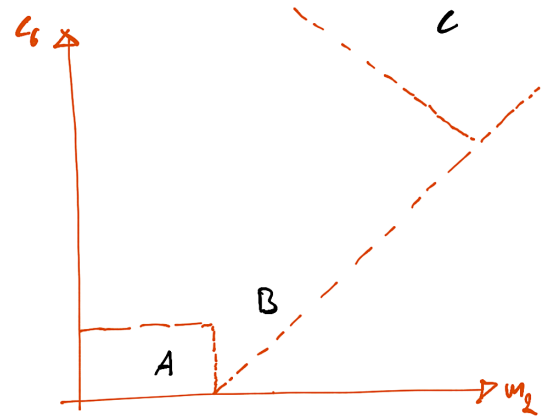

FIG. 1. Parameter space in the loosely bound Skyrme model with the BPS-Skyrme term. c_6 is the BPS-Skyrme term coefficient and m_2 is the coefficient of the loosely bound potential. The region A corresponds to a small BPS-Skyrme term and the region of parameter space that we will study in this paper. B corresponds to a large m_2 and medium-sized value of c_6. Finally, C corresponds to the near-BPS regime of the BPS-Skyrme model; in this regime, the kinetic term and the Skyrme term are small perturbations of the BPS-Skyrme model.

numerical calculations, as mentioned above. The region of parameter space to the right of the diagonal dashed line in the diagram corresponds to very large values of m_2 and leads to Skyrmions that lose the symmetries of platonic solids; in particular, the 4-Skyrmion loses its cubic symmetry which then becomes tetrahedral [27] and the model in turn loses its properties of nuclear clustering. The tendencies that we explore here in region A will make the motivations for studying region B in the future; as we will see in the affirmative.

Let us comment on the relation of the higher-order derivative terms with respect to the underlying QCD. As QCD at low energies is strongly coupled, a rigorous explicit derivation is extremely difficult to carry out. Nevertheless, the Skyrme term has been derived from the QCD Lagrangian using partial bosonization where only the phases of the fermions are bosonized [32]; this is done by gauging the flavor symmetry, however, this gauging does not survive quantization. A crucial point in this derivation is the claim that the quantum average of the fermion bilinear in QCD is the same as the quantum average in the partially bosonized action. The Skyrme term has been derived in Ref. [32] using this procedure and in principle higher-order terms can also be considered this way; in particular, the BPS-Skyrme term. This is, however, beyond the scope of the present paper. From a more phenomenologically point of view, the Skyrme term has been derived from an effective Lagrangian of vector mesons by integrating out the ρ meson [33]. The Skyrme action has also been derived as the low-energy effective action for the pions in the framework of the Sakai-Sugimoto model [34]; this model is however based

on string theory and is not directly related to QCD. The BPS-Skyrme term corresponds physically to integrating out the ω meson [35,36] due to the interaction giving rise to the $\omega \rightarrow \pi^+\pi^-\pi^0$ decay. To the best of our knowledge, there is no derivation of the loosely bound (quadratic) potential from QCD as of yet; it is included due to its ability to lower the classical binding energies.

The paper is organized as follows. In Sec. II, we present the model and units that we will be using in this paper. In Sec. III, we calculate all the observables that we will evaluate. Section IV shows the results of the numerical calculations and evaluation of the observables. Finally, Sec. V concludes with a discussion of the results found.

II. THE MODEL

The model under consideration is a generalized Skyrme model and the Lagrangian density in physical units reads

$$\mathcal{L} = \frac{f_\pi^2}{4}\mathcal{L}_2 + \frac{1}{e^2}\mathcal{L}_4 + \frac{4c_2c_6}{c_4^2 f_\pi^2 e^4}\mathcal{L}_6 - \frac{\tilde{m}_\pi^2 f_\pi^2}{4m_1^2}V, \quad (1)$$

where the kinetic (Dirichlet) term, Skyrme term [1,2], and BPS-Skyrme [18,19] term are given by

$$\mathcal{L}_2 = \frac{1}{4}\text{Tr}(L_\mu L^\mu), \quad \mathcal{L}_4 = \frac{1}{32}\text{Tr}([L_\mu, L_\nu][L^\mu, L^\nu]),$$

$$\mathcal{L}_6 = \frac{1}{144}\eta_{\mu\mu'}(\epsilon^{\mu\nu\rho\sigma}\text{Tr}[L_\nu L_\rho L_\sigma])(\epsilon^{\mu'\nu'\rho'\sigma'}\text{Tr}[L_{\nu'}L_{\rho'}L_{\sigma'}]), \quad (2)$$

and the left-invariant current is

$$L_\mu \equiv U^\dagger \partial_\mu U, \qquad R_\mu \equiv \partial_\mu U U^\dagger; \quad (3)$$

for later convenience, we also defined the right-invariant current R_μ. The constants are the following: f_π is the pion decay constant having units of energy (MeV), $e > 0$ is the dimensionless Skyrme-term coefficient, $c_6 > 0$ is the dimensionless BPS-Skyrme term coefficient, $\tilde{m}_\pi$ is the pion mass (in MeV), and, finally, m_1 is the dimensionless pion mass parameter. c_2 and c_4 are dimensionless constants that can be chosen arbitrarily; we will fix them shortly. $\mu, \nu, \rho, \sigma = 0, 1, 2, 3$ are spacetime indices, we are using the mostly positive metric signature and U is the Skyrme field which is related to the pions as

$$U = \mathbf{1}_2 \sigma + i\tau^a \pi^a, \quad (4)$$

with $\det U = 1$ being the nonlinear sigma model constraint, which is equivalent to $\sigma^2 + \pi^a \pi^a = 1$ and τ^a are the Pauli matrices.

We will now rescale the theory and work in (dimensionless) Skyrme units, following Ref. [31]. The lengths are rescaled as $\tilde{x}^i = \mu x^i$, where both $\tilde{x}^i$ and μ have units of inverse energy (MeV^{-1}), and, similarly, the energy is

rescaled as $\tilde{E} = \lambda E$, where $\tilde{E}$ and λ have units of energy (MeV). Finally, we get the dimensionless Lagrangian density

$$\mathcal{L} = c_2\mathcal{L}_2 + c_4\mathcal{L}_4 + c_6\mathcal{L}_6 - V, \quad (5)$$

where $c_2 > 0$ and $c_4 > 0$ are positive definite real constants and $c_6 \geq 0$ is a positive semidefinite real constant and the rescaling parameters are determined as

$$\lambda = \frac{f_\pi}{2e\sqrt{c_2c_4}}, \qquad \mu = \sqrt{\frac{c_2}{c_4}}\frac{2}{ef_\pi}, \quad (6)$$

whereas the pion mass in physical units (MeV) is given by

$$\tilde{m}_\pi = \frac{\sqrt{c_4}}{2c_2}ef_\pi m_1. \quad (7)$$

We have assumed in the above expression that the part of the potential V contributing to the pion mass is normalized to m_1 in dimensionless units.

A comment about the normalization chosen for the BPS-Skyrme term, $\mathcal{L}_6$, in this paper is in store. Derrick's theorem [37] implies that a higher-derivative term is necessary for stability of a soliton with finite size and energy. Skyrme used the simplest possibility, namely, a fourth-order derivative correction to stabilize the Skyrmion, but a sixth-order term like the BPS-Skyrme term can equally well stabilize the Skyrmion without the presence of the standard Skyrme term. This situation corresponds to $c_4 = 0$ and $c_6 > 0$, which however is not possible in our normalization and calibration of the energy and length units. As explained in the Introduction, in this paper, we focus on the region in parameter space where the BPS-Skyrme term is added as a perturbation to the loosely bound Skyrme model.

The potential we will use in this paper is composed by the loosely bound potential [30] and the standard pion mass term

$$V = V_1 + V_2, \quad (8)$$

where we have defined

$$V_n \equiv \frac{1}{n}m_n^2(1-\sigma)^n. \quad (9)$$

This is the part of the most general potential to second order in $\sigma = \text{Tr}[U]/2$ giving the lowest binding energies [31].

The Lagrangian density (5) without a potential, possesses $\text{SU}(2) \times \text{SU}(2)$ symmetry, which is explicitly broken to the diagonal $\text{SU}(2)$ by the potential (8). The latter $\text{SU}(2)$ corresponds to isospin, which we will keep unbroken in this paper.

The Skyrme field is a map from point-compactified 3-space $\mathbb{R}^3 \cup \{\infty\} \simeq S^3$ to the target space, $\text{SU}(2)$, characterized by the third homotopy group

$$\pi_3(\mathrm{SU}(2)) = \mathbb{Z} \ni B, \tag{10}$$

where B is the topological degree, also called the baryon number. The baryon number is the integral of the baryon charge density

$$B = \frac{1}{2\pi^2} \int d^3x \mathcal{B}^0, \tag{11}$$

with

$$\mathcal{B}^0 = -\frac{1}{12} \epsilon^{ijk} \mathrm{Tr}[L_i L_j L_k]. \tag{12}$$

Throughout the paper, we will use the short-hand notation B-Skyrmion for a Skyrmion with topological degree B.

For convenience, we allow for a generic normalization of the terms in the model. However, once we want to calibrate the model, we have to fix the choice of the coefficients c_2 and c_4. The standard choice of Skyrme units corresponds to setting $c_2 = c_4 = 2$ for which energies and lengths are given in units of $f_\pi/(4e)$ and $2/(ef_\pi)$, respectively [38]. In this paper, we will adhere to the convention used in Refs. [30,31], i.e.,

$$c_2 = \frac{1}{4}, \qquad c_4 = 1, \tag{13}$$

for which, according to Eq. (6), energies and lengths are given in units of f_π/e and $1/(ef_\pi)$, respectively. The pion mass in physical units is

$$\tilde{m}_\pi = \frac{\sqrt{c_4}}{2c_2} ef_\pi \sqrt{-\frac{\partial V}{\partial \sigma}}\bigg|_{\sigma=1} = 2ef_\pi m_1, \tag{14}$$

where we have used the normalization (13) in the last equality. The pion mass $m = 1$ used in Ref. [13], corresponds to $m_1 = 1/4$ and in turn, $\tilde{m}_\pi = ef_\pi/2$ in our units and normalization.

III. OBSERVABLES

We have now defined the model, set the notation, and we are ready to calculate the expressions for the observables that we will determine numerically and compare to experimental data. We will follow Ref. [31] and calculate Skyrmions of baryon numbers one and four; this choice is advantageous for several reasons: the importance of the 4-Skyrmion ($B = 4$) as it corresponds to the alpha particle and plays a crucial role in nuclear clustering; the ground state of ^{4}He is a spin-0, isospin-0 state, which means that it is determined by the classical energy of the 4-Skyrmion, and finally, the 1-Skyrmion represents the nucleon/proton/ neutron in the theory with unbroken isospin, and therefore, we can use this for comparison with experimental data for the proton.

The 1-Skyrmion is spherically symmetric and hence is described by the hedgehog ansatz

$$U^{(1)} = \mathbf{1}_2 \cos f(r) + i\hat{x}^a \tau^a \sin f(r), \tag{15}$$

where $r = \sqrt{(x^1)^2 + (x^2)^2 + (x^3)^2}$ is the radial coordinate and $\hat{x}^a = x^a/r$ is the spatial unit 3-vector. The classical energy for the 1-Skyrmion is given by plugging the above ansatz into the Lagrangian (5) yielding

$$\begin{aligned}
E_1 &= -\int d^3x \mathcal{L}[U^{(1)}] \\
&= 4\pi \int dr r^2 \bigg[c_2 \left(\frac{1}{2} f_r^2 + \frac{1}{r^2} \sin^2 f \right) \\
&\quad + c_4 \frac{\sin^2 f}{r^2} \left(f_r^2 + \frac{\sin^2 f}{2r^2} \right) + c_6 \frac{\sin^4(f) f_r^2}{r^4} \\
&\quad + m_1^2 (1 - \cos f) + \frac{1}{2} m_2^2 (1 - \cos f)^2 \bigg],
\end{aligned} \tag{16}$$

where $f_r \equiv \partial_r f$.

A. Calibration

In this paper, we choose like in Refs. [30,31] to calibrate the model by fitting the mass and the size of ^{4}He to those of the $B = 4$ Skyrmion. Since the numerical calculations in the $B = 4$ sector are numerically expensive, we choose to use the rational map approximation to estimate the mass and size of the 4-Skyrmion. It is known that in the standard Skyrme model, the rational map approximation provides quick solutions within about 1% accuracy [8,9]. This will, however, be the first time it is used in the loosely bound Skyrme model; we will therefore check the results in the $c_6 = 0$ sector by comparing to the full PDE solutions of Ref. [31].

The rational map is made by performing a radial suspension of the Skyrme field

$$U^{(\mathrm{RM})} = \mathbf{1} \cos f + i\tau^a n^a \sin f, \tag{17}$$

where n^a is a unit 3-vector. The suspension means choosing $f(r)$ and $n(\theta, \phi)$ in normal spherical coordinates. It will however be convenient to use the complex coordinate $z = e^{i\phi} \tan\frac{\theta}{2}$ on the Riemann sphere, for which the 2-sphere reads

$$n^1 = \frac{z + \bar{z}}{1 + |z|^2}, \quad n^2 = \frac{i(\bar{z} - z)}{1 + |z|^2}, \quad n^3 = \frac{1 - |z|^2}{1 + |z|^2}. \tag{18}$$

The generalization to a degree B map on the Riemann sphere is then made by using the rational map $R(z)$, which is a holomorphic function of z and the 3-vector thus reads [9]

$$n^1 = \frac{R(z) + \bar{R}(\bar{z})}{1 + |R(z)|^2}, \qquad n^2 = \frac{i(\bar{R}(\bar{z}) - R(z))}{1 + |R(z)|^2}, \qquad n^3 = \frac{1 - |R(z)|^2}{1 + |R(z)|^2}. \qquad (19)$$

We can now write our static Lagrangian density as [9,18,19,39]

$$-\mathcal{L}[U^{(\mathrm{RM})}] = c_2 \left(\frac{1}{2} f_r^2 + \frac{\sin^2 f}{r^2} \frac{(1 + |z|^2)^2}{(1 + |R|^2)^2} |R_z|^2 \right) + c_4 \frac{\sin^2 f}{r^2} \left(f_r^2 \frac{(1 + |z|^2)^2}{(1 + |R|^2)^2} |R_z|^2 + \frac{\sin^2 f}{2r^2} \frac{(1 + |z|^2)^4}{(1 + |R|^2)^4} |R_z|^4 \right)$$

$$+ c_6 \frac{\sin^4(f) f_r^2}{r^4} \frac{(1 + |z|^2)^4}{(1 + |R|^2)^4} |R_z|^4 + m_1^2(1 - \cos f) + \frac{1}{2} m_2^2 (1 - \cos f)^2, \qquad (20)$$

which by integration over 3-space gives

$$E_B^{(\mathrm{RM})} = -\int d^3x \mathcal{L}[U^{(\mathrm{RM})}]$$

$$= 4\pi \int dr \left[c_2 \left(\frac{1}{2} r^2 f_r^2 + B\sin^2 f \right) \right.$$

$$+ c_4 \sin^2 f \left(B f_r^2 + \mathcal{I} \frac{\sin^2 f}{2r^2} \right) + c_6 \mathcal{I} \frac{\sin^4(f) f_r^2}{r^2}$$

$$\left. + m_1^2 (1 - \cos f) + \frac{1}{2} m_2^2 (1 - \cos f)^2 \right], \qquad (21)$$

where

$$\mathcal{I} \equiv \frac{1}{4\pi} \int \frac{2i dz \wedge d\bar{z}}{(1 + |z|^2)^2} \left(\frac{1 + |z|^2}{1 + |R|^2} R_z \right)^4. \qquad (22)$$

For the 4-Skyrmion, the minimizing rational map has the form [8]

$$R(z) = \frac{z^4 + i2\sqrt{3}z^2 + 1}{z^4 - i2\sqrt{3}z^2 + 1}, \qquad (23)$$

which upon integration gives $\mathcal{I}_4 \simeq 20.6496$.

With the (rational map) approximated solution for the cubic 4-Skyrmion, we can now perform the calibration by calculating the mass and size of the solution. Since, as we mentioned already, the ground state of $^4\mathrm{He}$ is a spin-0, isospin-0 state, the mass does not receive a contribution from spin-isospin quantization and is thus given by the classical static energy (21). The electric charge density is given by $\rho_E = \frac{1}{2} \frac{1}{2\pi^2} \mathcal{B}^0 + \mathcal{I}^3$ [5], but since the isospin-0 state does not contribute to the charge density, the charge radius is determined only from the baryon charge density

$$\mathcal{B}^0 = -\frac{B\sin^2(f) f_r}{r^2}, \qquad (24)$$

which yields the baryon charge and electric charge radii (squared)

$$r_4^2 = r_{E,4}^2 = -\frac{2}{\pi} \int dr r^2 \sin^2(f) f_r, \qquad (25)$$

where f is a minimizer of the energy (21) with the rational map (23), and we have normalized the integral by dividing with $B/2$.

We can finally determine the parameters of the model as

$$f_\pi = 2\sqrt{c_2} \sqrt{\frac{r_{E,4} M_{^4\mathrm{He}}}{r_{^4\mathrm{He}} E_4}}, \qquad e = \frac{1}{\sqrt{c_4}} \sqrt{\frac{r_{E,4} E_4}{r_{^4\mathrm{He}} M_{^4\mathrm{He}}}}, \qquad (26)$$

which simplifies with the convention (13) to

$$f_\pi = \sqrt{\frac{r_{E,4} M_{^4\mathrm{He}}}{r_{^4\mathrm{He}} E_4}}, \qquad e = \sqrt{\frac{r_{E,4} E_4}{r_{^4\mathrm{He}} M_{^4\mathrm{He}}}}, \qquad (27)$$

where it is understood that $r_{E,4} = \sqrt{r_{E,4}^2}$ and the values of the experimental data used are $M_{^4\mathrm{He}} = 3727$ MeV and $r_{^4\mathrm{He}} = 8.492 \times 10^{-3}$ MeV^{-1}.

B. Mass spectrum

We are now ready to calculate the mass spectrum; the first mass we need is the mass of the nucleon. It has two contributions: the (classical) soliton mass, E_1 [see Eq. (16)], and that coming from spin-isospin quantization, ϵ_1 which we will now calculate.

The quantum contribution from spin-isospin quantization can be calculated from the kinetic part of the Lagrangian (5), as follows:

$$T = \frac{1}{2} a_i U_{ij} a_j = \Lambda \mathrm{Tr}[\dot{A}\dot{A}^\dagger], \qquad a_i \equiv -i\mathrm{Tr}(\tau^i A^\dagger \dot{A}). \qquad (28)$$

Because of spherical symmetry of the nucleon, we get $U_{ij} = \Lambda \delta_{ij}$ with [5,40,41]

$$\Lambda = \frac{8\pi}{3} \int dr r^2 \sin^2 f \left[c_2 + c_4 f_r^2 + \frac{c_4}{r^2} \sin^2 f + \frac{2c_6 \sin^2(f) f_r^2}{r^2} \right]. \qquad (29)$$

Since $\text{Tr}[\dot{A}\dot{A}^{\dagger}]$ is the kinetic term on the 3-sphere, the quantization thereof yields

$$T = \frac{1}{8\Lambda}\ell(\ell+2) = \frac{1}{2\Lambda}J(J+1), \tag{30}$$

where $J = \ell/2$ is the spin quantum number. Finally, the spin contribution for the spin-1/2 ground state of the nucleon reads

$$T_{1/2} = \frac{1}{2\Lambda}\frac{3}{4}, \tag{31}$$

and in physical units

$$\tilde{m}_N = \tilde{E}_1 + \tilde{\epsilon}_1 = \frac{f_\pi}{e}E_1 + \frac{3e^3 f_\pi}{8\Lambda}. \tag{32}$$

Now we can quickly get the mass of the Delta resonance, by setting $J = 3/2$, and hence, we get

$$\tilde{m}_\Delta = \tilde{E}_1 + 5\tilde{\epsilon}_1. \tag{33}$$

The final mass that we will calculate and compare to data in this paper is the pion mass, which is given in physical units in Eq. (14).

C. Binding energy

One of the prime observables in this paper is the binding energy. The classical and total binding energies are defined as

$$\Delta_B = BE_1 - E_B, \qquad \Delta_B^{\text{tot}} = B(E_1 + \epsilon_1) - E_B - \epsilon_B, \tag{34}$$

and the relative classical and total binding energies in turn read

$$\delta_B = 1 - \frac{E_B}{BE_1}, \qquad \delta_B^{\text{tot}} = 1 - \frac{E_B + \epsilon_B}{B(E_1 + \epsilon_1)}, \tag{35}$$

respectively. Notice that the quantum contribution to the B-Skyrmion, ϵ_B, *lowers* the total binding energy, whereas

the quantum contribution to the 1-Skyrmion *raises* the total binding energy. In particular, for the 4-Skyrmion, the ground state is a spin-0, isospin-0 state, and thus the quantum contribution vanishes, i.e., $\epsilon_4 = 0$, yielding the relative total binding energy

$$\delta_4^{\text{tot}} = 1 - \frac{E_4}{B(E_1 + \epsilon_1)}. \tag{36}$$

This means that for the 4-Skyrmion, the spin-isospin quantization only exacerbates the problem of the binding energy being too large.

D. Charge radii

We will now calculate the baryon charge radius of the nucleon and the electric charge radius of the proton. We begin by calculating the vectorial current. The infinitesimal transformation

$$U \to U + i\theta_V^a[Q^a, V], \tag{37}$$

thus gives rise to the vectorial current

$$
\begin{aligned}
J_V^{\mu a} = & \frac{ic_2}{2}\text{Tr}[(R^\mu - L^\mu)Q^a] \\
& + \frac{ic_4}{8}\text{Tr}[([R_\nu,[R^\mu,R^\nu]] - [L_\nu,[L^\mu,L^\nu]])Q^a] \\
& + \frac{ic_6}{24}\eta_{\nu\nu'}\epsilon^{\nu'\rho'\sigma'\tau'}\text{Tr}[L_{\rho'}L_{\sigma'}L_{\tau'}] \\
& \times \epsilon^{\nu\rho\sigma\mu}\text{Tr}[(R_\rho R_\sigma - L_\rho L_\sigma)Q^a], \tag{38}
\end{aligned}
$$

whose integrated zeroth component for the hedgehog ansatz (15), can be written as

$$
\begin{aligned}
\int d^3 x J_V^{0a} = & -\frac{i8\pi}{3}\int dr[c_2 r^2\sin^2 f + c_4\sin^2 f(\sin^2 f + r^2 f_r^2) \\
& + 2c_6\sin^4(f)f_r^2]\text{Tr}[\tau^a \dot{A}A^{\dagger}],
\end{aligned}
$$

from which we can construct the electric (radial) density as [5]

$$
\begin{aligned}
\int d\Omega \rho_E &= \int d\Omega\left(\frac{1}{2}\frac{1}{2\pi^2}\mathcal{B}^0 + \mathcal{I}^3\right) \\
&= -\frac{\sin^2(f)f_r}{\pi r^2} + \frac{c_2\sin^2 f + \frac{c_4}{r^2}\sin^2(\sin^2 f + r^2 f_r^2) + \frac{2c_6}{r^2}\sin^4(f)f_r^2}{2\int dr(c_2 r^2\sin^2 f + c_4\sin^2(\sin^2 f + r^2 f_r^2) + 2c_6\sin^4(f)f_r^2)},
\end{aligned}
\tag{39}
$$

where we have used $Q^a = \tau^a/2$. The above radial function is the charge density of the proton, and it integrates to unity, i.e., $\int dr r^2 \rho_E = 1$ (as it should). We can thus construct the electric charge radius (squared) as

$$r_{E,1}^2 = \int dr r^4 \rho_E, \tag{40}$$

whereas the baryon charge radius is given by

$$r_1^2 = -\frac{2}{\pi} \int dr r^2 \sin^2(f) f_r. \qquad (41)$$

E. Axial coupling

In this paper, we will consider the axial coupling [5], in addition to the ones considered in Ref. [31]. The axial current reads

$$
\begin{aligned}
J_A^{\mu a} =& \frac{ic_2}{2} \mathrm{Tr}[(R^\mu + L^\mu)Q^a] \\
&+ \frac{ic_4}{8} \mathrm{Tr}[([R_\nu,[R^\mu,R^\nu]] + [L_\nu,[L^\mu,L^\nu]])Q^a] \\
&+ \frac{ic_6}{24} \eta_{\nu\nu'} \epsilon^{\nu'\rho'\sigma'\tau'} \mathrm{Tr}[L_{\rho'}L_{\sigma'}L_{\tau'}] \\
&\times \epsilon^{\nu\rho\sigma\mu} \mathrm{Tr}[(R_\rho R_\sigma + L_\rho L_\sigma)Q^a],
\end{aligned} \qquad (42)
$$

corresponding to the infinitesimal transformation

$$U \to U + i\theta_A^a \{Q^a, U\}. \qquad (43)$$

Imposing spherical symmetry and ignoring second order in time derivatives, we can write

$$\int d^3 x J_{Ai}^a = \frac{g_A}{2} \mathrm{Tr}[\tau^i A^\dagger \tau^a A], \qquad (44)$$

where the axial coupling is given by[3]

$$
\begin{aligned}
g_A =& -\frac{4\pi}{3} \int dr r \Big[c_2(\sin 2f + r f_r) \\
&+ c_4 \left(\frac{\sin^2 f \sin 2f}{r^2} + \frac{2\sin^2(f) f_r}{r} + \sin(2f) f_r^2 \right) \\
&+ \frac{2c_6 \sin^2 f}{r^2} \left(\frac{\sin^2(f) f_r}{r} + \sin(2f) f_r^2 \right) \Big],
\end{aligned} \qquad (45)
$$

and we have used $Q^a = \tau^a/2$. Although the axial coupling is dimensionless, it is still in Skyrme units, and so to relate to its experimentally observed value, we need to change the units back to physical units

$$\tilde{g}_A = \frac{g_A}{e^2 c_4} = \frac{g_A}{e^2} \qquad (46)$$

by multiplying the result by $\lambda\mu = 1/(e^2 c_4)$, and in the last equality, we have used the convention of Eq. (13), which sets $c_4 = 1$.

---

[3]Although the contributions to the axial coupling from the terms up to sixth order in derivatives have been calculated in Refs. [40,41], our expression does not agree with that of the latter references. However, our expression agrees with that of Ref. [5] up to fourth-order derivative terms.

IV. RESULTS

We have now presented the loosely bound Skyrme model with up to six orders of derivative terms and the observables that we will compare to experimental data. Now we just need to calculate the numerical solutions of the Skyrmion profile functions for the 1-Skyrmion and the 4-Skyrmion, respectively, in order to evaluate the observables presented in Sec. III. We calculate the radial ODEs for the Skyrmion profile functions using the relaxation method and show the results below.

A. Binding energies

We will start by presenting the relative classical and total binding energies in Figs. 2 and 3, respectively. In these and the remaining figures containing contour plots in this section, panel (a) shows the (m_2, c_6) plane of parameter space for fixed $m_1 = 0.25$ and (b) shows the (m_1, c_6) plane for $m_2 = 0.7$.

We see—as expected from Ref. [31]—that the binding energy decreases when m_2 is turned on and monotonically decreases until $m_2 = 0.8$, which is the upper bound for $c_6 = 0$ for which the cubic symmetry of the 4-Skyrmion is still retained. Now we turn on the BPS-Skyrme term (whose coefficient is c_6), and we can see that for $m_2 = 0$, it first increases the binding energy until a plateau quickly is reached. Interestingly, however, when $m_2 = 0.8$, the BPS-Skyrme term decreases the binding energy and so much so that the classical binding energy in Fig. 2(a) [Fig. 2(b)] turns negative in the top-right (top-left) corner of the graph. We should warn the reader that since we are using the rational map approximation for the 4-Skyrmion, the energy is expected to be overestimated by about 1%–2%, and since the 1-Skyrmion is an exact numerical solution, this translates into a 1%–2% underestimation of the binding energy. Therefore, the contour line marking $\delta_4 = 0$ actually corresponds to a classical binding energy of about 1%–2%. Shortly, we will estimate the systematic error by making a comparison to the results of Ref. [31].

Figure 2(b) shows the (m_1, c_6) plane of parameter space for fixed $m_2 = 0.7$. It is a little surprising that the increase of the pion mass m_1 leads to a slight increase in the binding energy. The conclusions in both Refs. [30] and [31] were that a larger pion mass was useful because it was possible to reach smaller binding energies. It is perfectly consistent, because the smaller binding energies were reached by increasing the coefficient of the loosely bound potential, m_2, and larger values of m_1 allow for larger values of m_2 before the cubic symmetry of the 4-Skyrmion is lost. For fixed m_2, however, an increase in the pion mass is observed not to help.

Taking the quantum contribution from spin-isospin quantization into account gives us the total binding energy of the 4-Skyrmion, i.e., δ_4^{tot}, shown in Fig. 3. Exactly the same tendencies can be seen in the total binding energies as
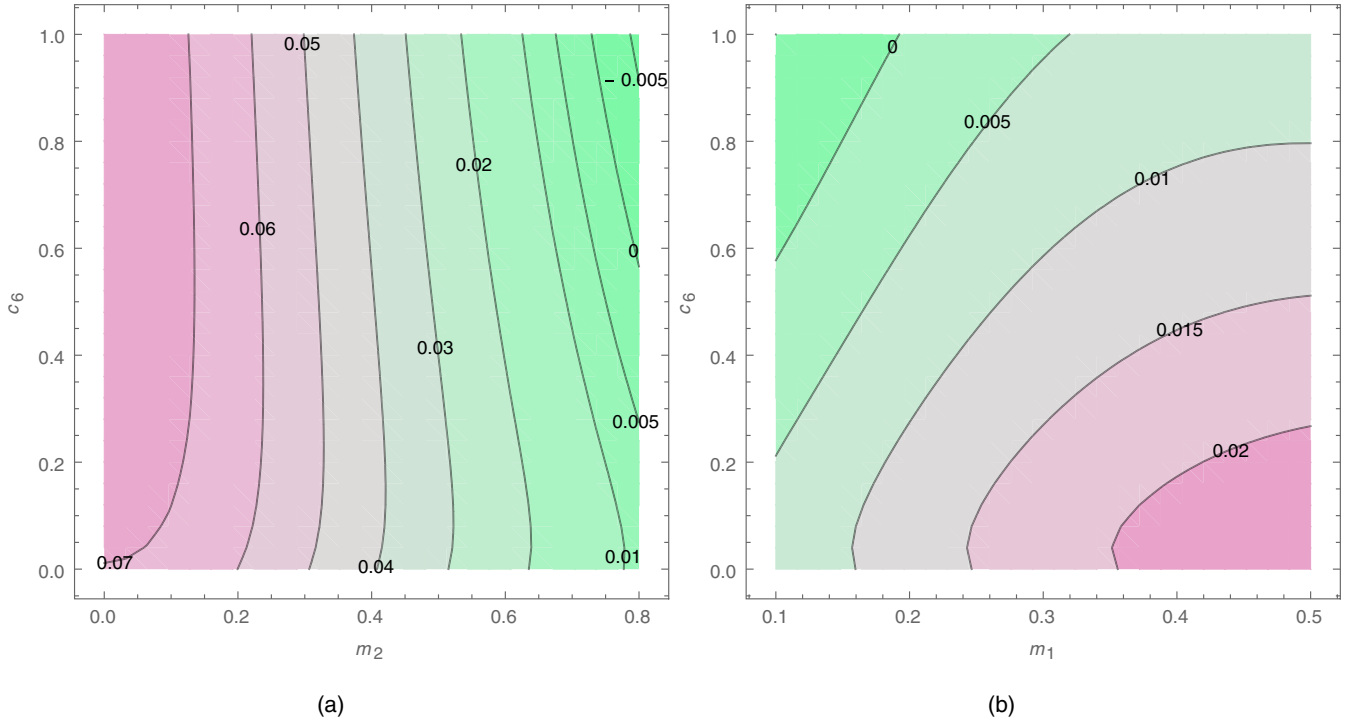
FIG. 2. Relative classical binding energy, δ_4, in (a) the (m_2, c_6) plane for $m_1 = 0.25$ and (b) the (m_1, c_6) plane for $m_2 = 0.7$.

in the classical binding energies. The lowest total binding energy in Fig. 3(a) is $\delta_4^{\text{tot}} = 3.03\%$ at $(m_2, c_6) = (0.8, 1)$ and marginally less at $(m_1, c_6) = (0.1, 1)$, see Figs. 3(a) and 3(b), respectively. Recall however, that due to the systematic error in using the rational map approximation,

the true total binding energy is expected to be about 1%–2% higher.

Let us now address the systematic error in the binding energy due to the rational map approximation. We take the binding energies calculated from the full PDE solutions in
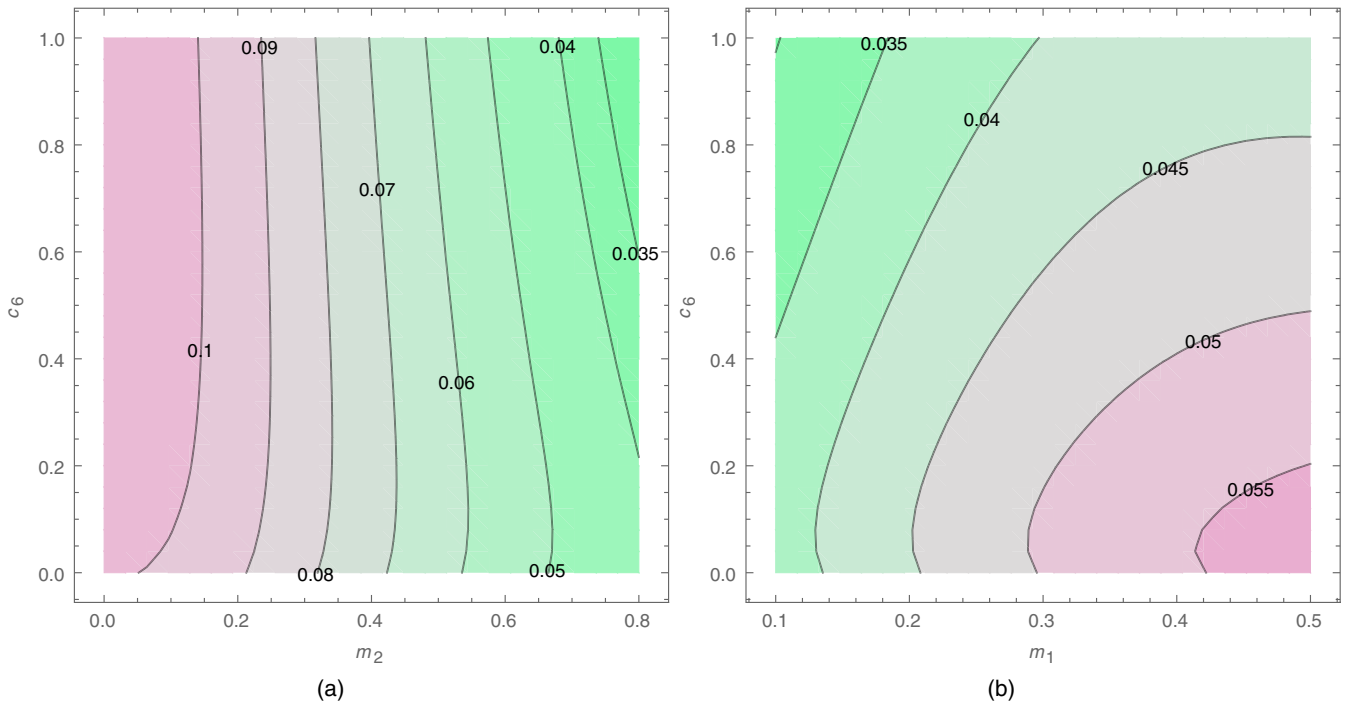
FIG. 3. Relative total binding energy, δ_4^{tot}, in (a) the (m_2, c_6) plane for $m_1 = 0.25$ and (b) the (m_1, c_6) plane for $m_2 = 0.7$.

Ref. [31] and compare them to the slice in our parameter space where $c_6 = 0$. Using a linear function in m_2, we will fit the difference between the full PDE solutions and the rational map approximations

$$\delta_4^{\text{corrected}} = \delta_4 + a + bm_2, \qquad (47)$$

where the constants are determined as $a = 0.01538$ and $b = 0.01142$. We also find that the dependence of m_1 of the difference is an order of magnitude smaller than that of m_2 and so we will ignore it here. Figure 4 shows the full PDE calculation as blue circles, the rational map approximation as the red dashed line and finally, the corrected relative binding energy of Eq. (47) as the green solid line. The linear fit tells us that the energy of the 4-Skyrmion is *indeed* overestimated, which in turn, underestimates the binding energy by 1.5% for $m_2 = 0$ and by 2.5% for $m_2 = 0.8$.

We used the classical binding energy to fit the correction for the systematic error of using the rational map approximation, and as we can see in Fig. 4(a), the linear correction works very well. Using the same correction, we can see in Fig. 4(b), that the corrected rational map approximation *overestimates* the true binding energy by a little. Nevertheless, with the correction for the systematic error, the relative classical binding energy matches the full PDE calculation within 0.0042%–0.065%, whereas the relative total binding energies only matches the PDEs within 0.18%–0.29%.

Finally, we will correct the systematic error of using the rational map approximation based on the above fit and show the relative total binding energy in Fig. 5.

Interestingly, we can see that the BPS-Skyrme term helps decreasing the binding energy for large m_2 and at the top-right corner of Fig. 5(a), we have about 5.5% binding energy and in the top-left corner of Fig. 5(b), it is about

5.3%. Compared to turning off the BPS-Skyrme term ($c_6 = 0$), the latter two values read 6.6% and 6.1%, respectively. With the results of Ref. [31] in mind, we expect that instead of decreasing the pion mass, increasing it and in the same time increasing also m_2, but beyond the values explored here, we will be able to reach even lower binding energies.

B. Calibration

In the calculation of the quantum contribution, which is an ingredient in the binding energies discussed above, the calibration of the model of the 4-Skyrmion to ^{4}He, has been used, see Eq. (27). Although the relative binding energy does not depend on the pion decay constant, f_π, other observables like the pion mass do depend on it. In Fig. 6, is shown the pion decay constant in the explored parameter space. We can see that increasing either the pion mass, m_1, or the coefficient of the loosely bound potential, m_2, with the other one held fixed, decreases the already too small pion decay constant. For large $m_2 \sim 0.8$, the pion decay constant in the model comes out as low as 67.5 MeV, compared to the experimental value of about 186 MeV; a factor of 3 too low.

The next parameter is the Skyrme-term coefficient e, which to the best of our knowledge is not experimentally determined. The calibration determines its value, which is shown in Fig. 7.

The general tendency of turning on the BPS-Skyrme term is an increase in e. Let us recall that the prefactor of the quantum correction to the energy of the 1-Skyrmion has an e^4 relative to its classical value. This naively implies that larger e leads to larger binding energies. As we know from Eq. (46), a larger e will also have the effect of decreasing the axial coupling, which we will see shortly is a desired feature.
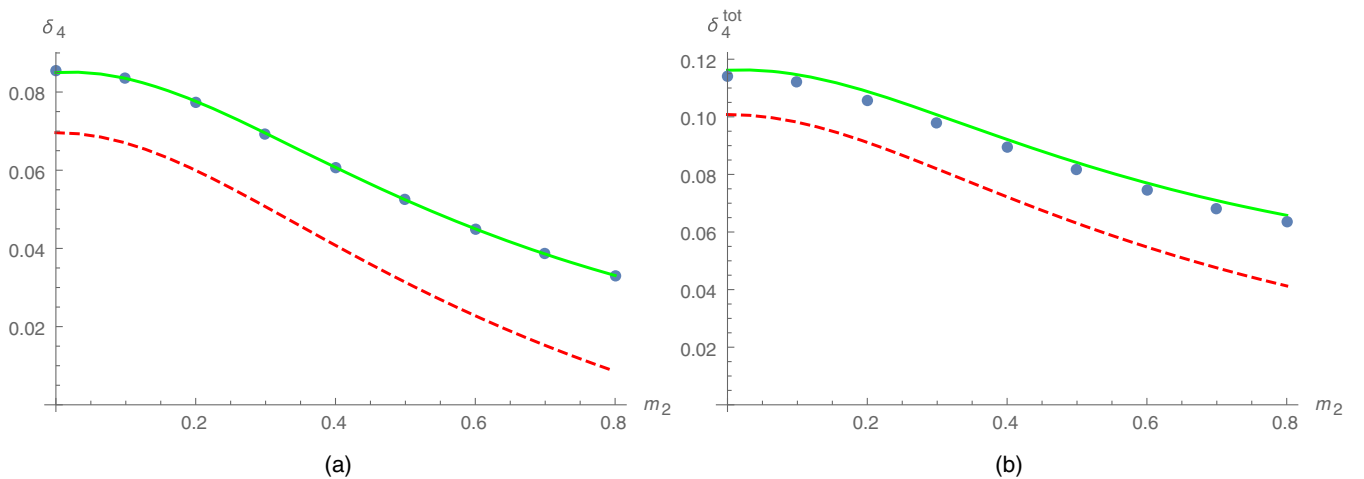

FIG. 4. Relative (a) classical and (b) total binding energy, δ_4 and δ_4^{tot}, as functions of m_2 for $m_1 = 0.25$. The blue circles are full PDE calculations from Ref. [31], the red dashed line is the calculation using the rational map approximation, and finally, the green solid line is the rational map approximation with a correction for systematic error, see Eq. (47).
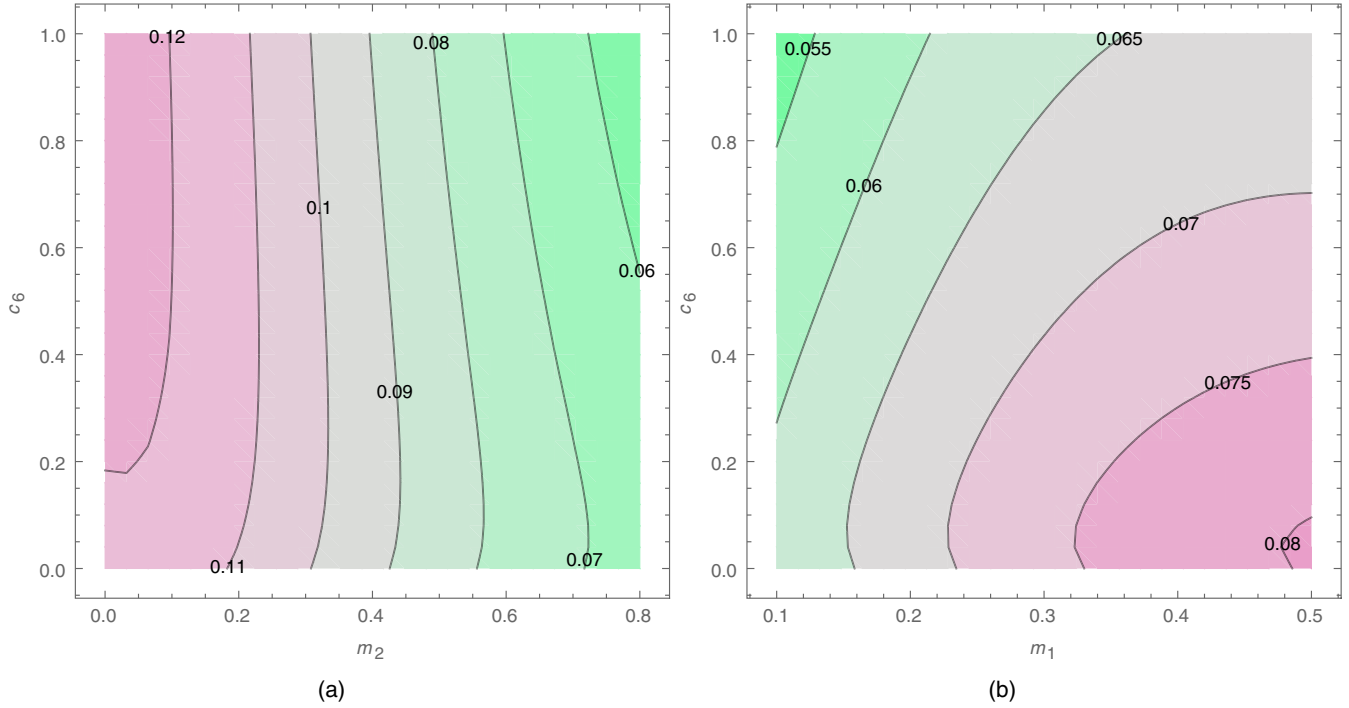
FIG. 5.   Relative total binding energy with a linear correction of the systematic error due to the rational map approximation, $\delta_4^{\text{corrected}}$, in (a) the (m_2, c_6) plane for $m_1 = 0.25$ and (b) the (m_1, c_6) plane for $m_2 = 0.7$.

C. Mass spectrum

We are now ready to calculate the physical spectrum, which we limit to the nucleon mass, the mass of the Delta resonance, and the pion mass. The nucleon mass is shown in Fig. 8. Recall that we calibrate the model by setting the mass of the 4-Skyrmion equal to the mass of helium-4.

We can see from Fig. 8(a) that increasing the loosely bound potential, decreases the nucleon mass, but yet not enough to reach its experimentally measured value around
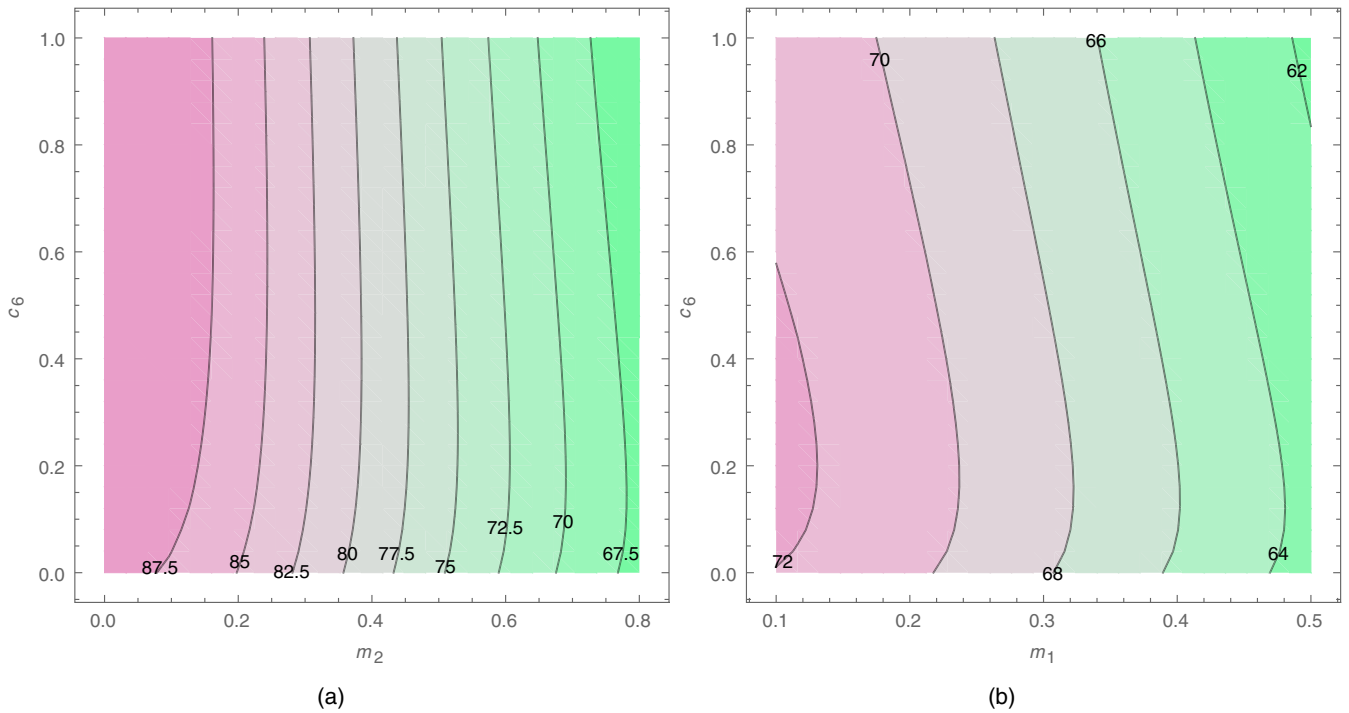
FIG. 6.   Pion decay constant, f_π [MeV], in (a) the (m_2, c_6) plane for $m_1 = 0.25$ and (b) the (m_1, c_6) plane for $m_2 = 0.7$.
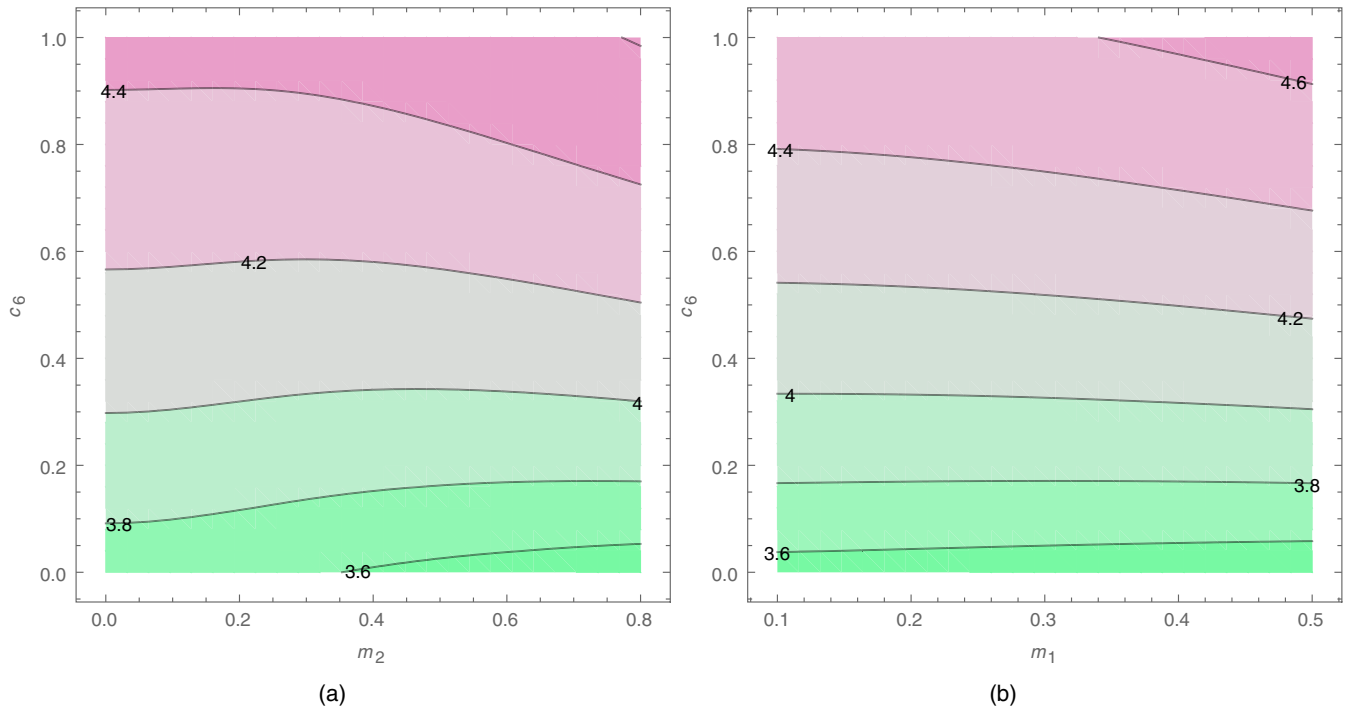
FIG. 7.   Skyrme term coefficient, e, in (a) the (m_2, c_6) plane for $m_1 = 0.25$ and (b) the (m_1, c_6) plane for $m_2 = 0.7$.

939 MeV. Similarly to the relative binding energy, when $m_2 = 0$ the BPS-Skyrme term initially increases the nucleon mass until a plateau quickly is reached. However, when m_2 is large the BPS-Skyrme term decreases the value of the nucleon mass. It is interesting to see from Fig. 8(b), that a smaller pion mass gives rise to a smaller

nucleon mass. The part of parameter space we considered here generally overestimates the nucleon mass.

We now turn to the mass of the Delta resonance, which is shown in Fig. 9. It is well-known that the Skyrme model generally underestimates it, and our flavor of the Skyrme model is no exception in this part of the parameter space.
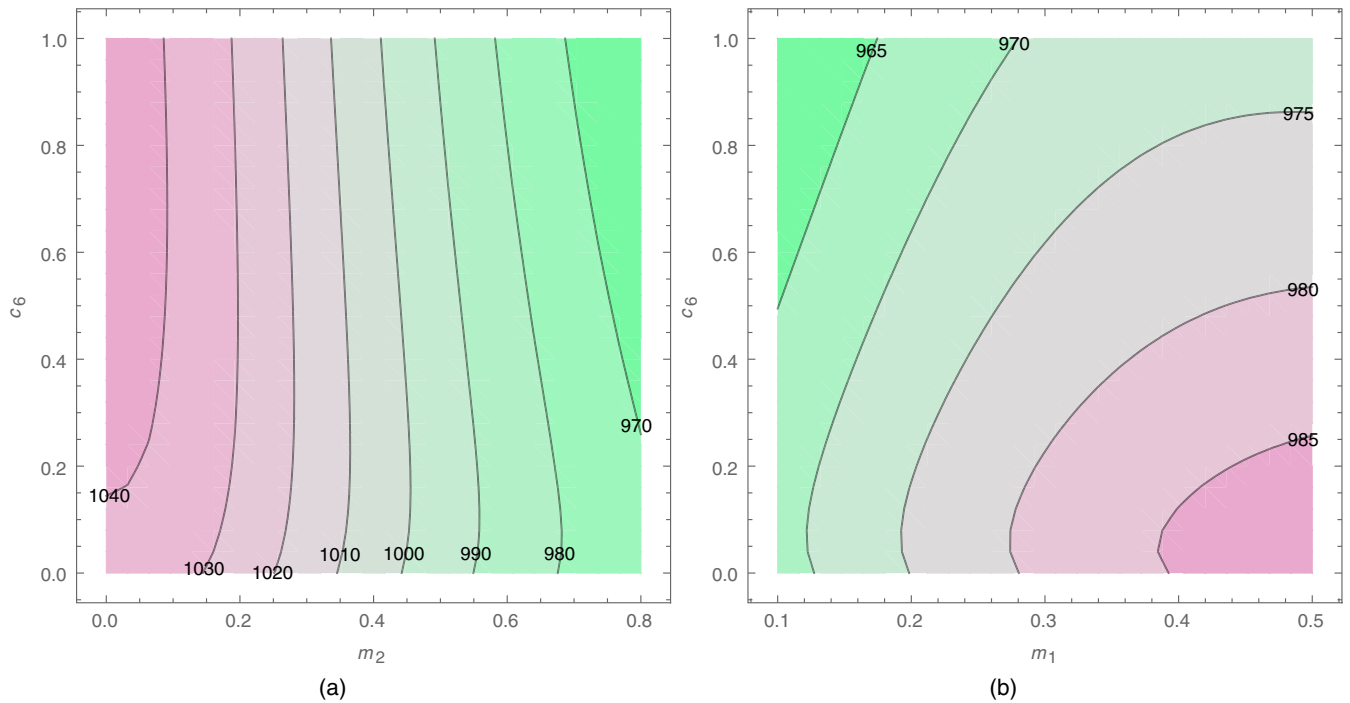

FIG. 8.   Nucleon mass, $\tilde{m}_N$ [MeV], in (a) the (m_2, c_6) plane for $m_1 = 0.25$ and (b) the (m_1, c_6) plane for $m_2 = 0.7$.
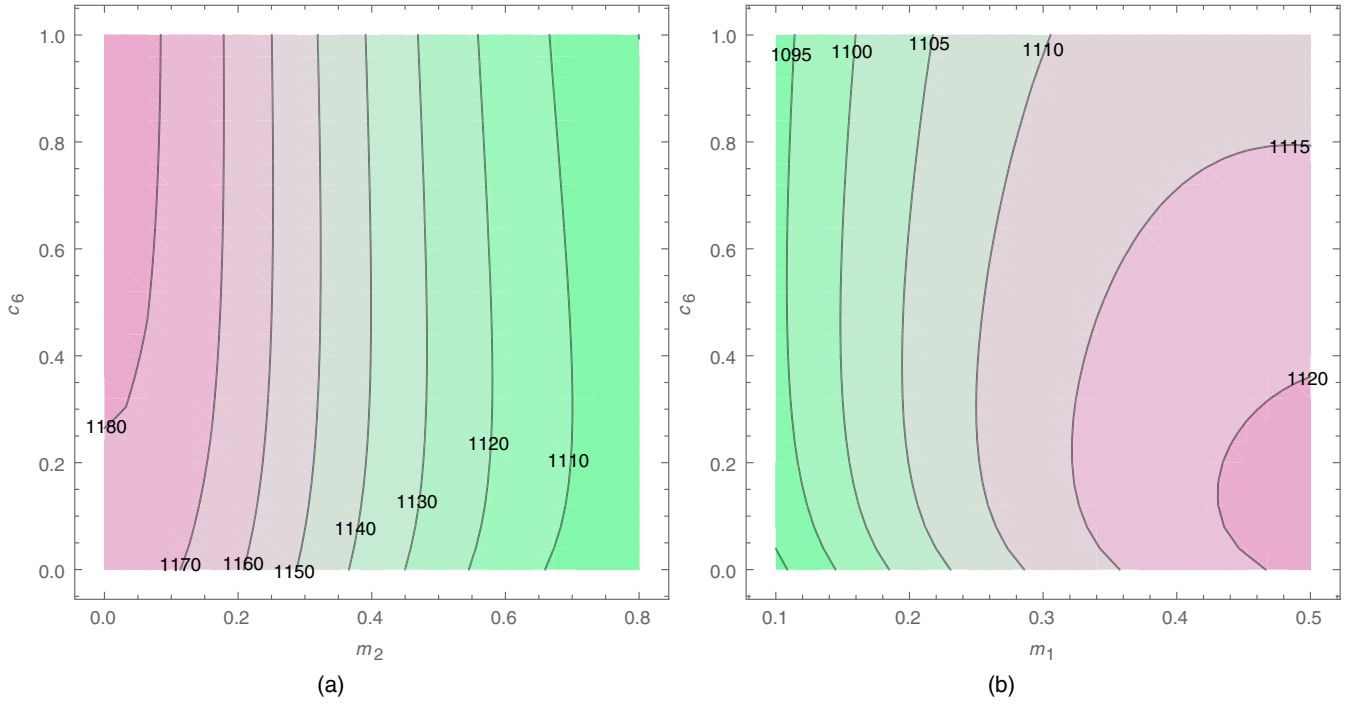
FIG. 9.   Mass of the Δ resonance, $\tilde{m}_\Delta$ [MeV], in (a) the (m_2, c_6) plane for $m_1 = 0.25$ and (b) the (m_1, c_6) plane for $m_2 = 0.7$.

The tendency of improvement of the binding energy and nucleon mass for larger values of the loosely bound potential (m_2) leads, however, to an exacerbation of the mass of the Delta resonance being too small.

The value of the pion mass is shown in Fig. 10. This is the first observable hitting spot-on the experimentally measured value. Of course the charged pions in nature are slightly heavier than the neutral one, but since we leave
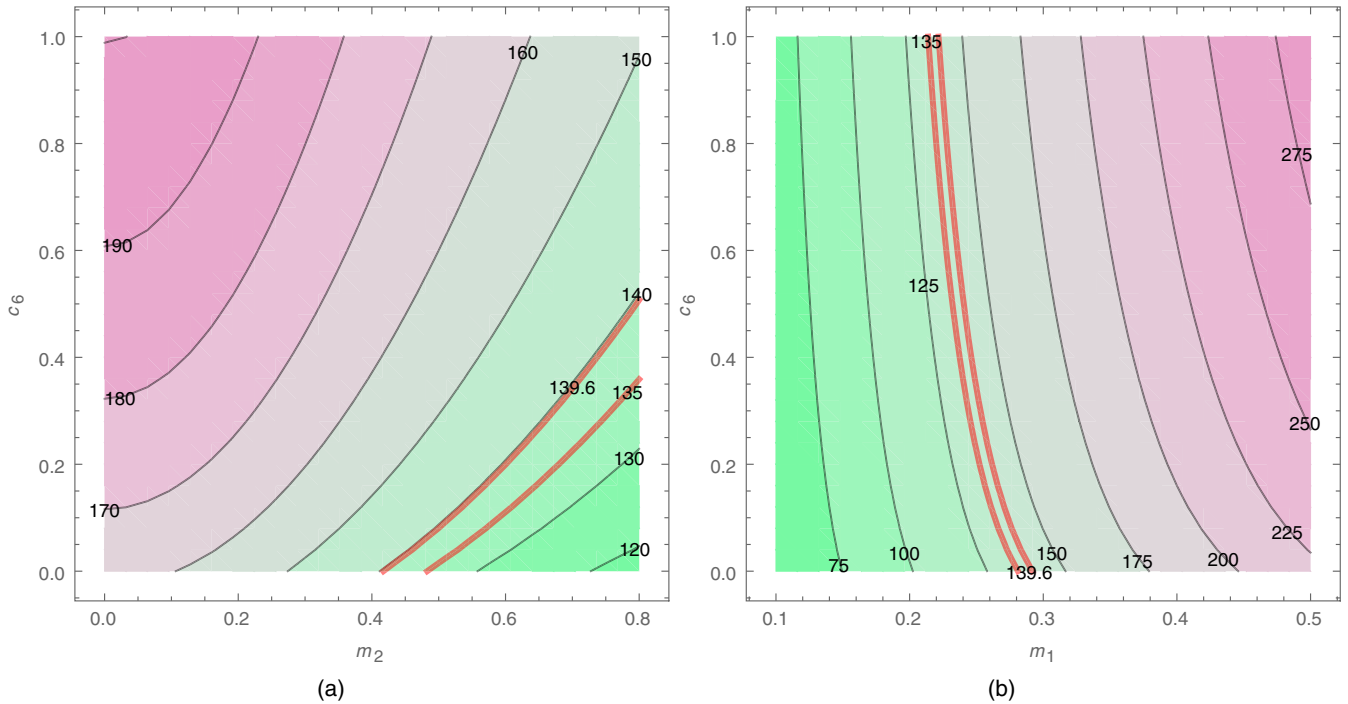

FIG. 10.   Pion mass, $\tilde{m}_\pi$ [MeV], in (a) the (m_2, c_6) plane for $m_1 = 0.25$ and (b) the (m_1, c_6) plane for $m_2 = 0.7$. The two bold red lines indicate the physical values of the pion masses.

chiral symmetry unbroken, all 3 pions are mass degenerate in our model. We can see that in order to hit the right experimental value and in the same time reduce the binding energy by turning on the BPS-Skyrme term, we need to reduce the value of the pion mass, m_1. However, the BPS-Skyrme term is expected to bind the constituents of the 4-Skyrmion more tightly, whereas the loosely bound potential repels them from each other. Therefore, we expect that it will be possible to increase the value of m_2 for medium/large values of c_6, and so the tendency of the model matching the experimental value of the pion mass is right on track.

Let us, however, remark that the pion decay constant is about a factor of 3 too small compared with experiment, and in the modern point of view in the Skyrme model, we accept this fact as the pion decay constant in the model being simply a renormalized value in the effective field theory and in the baryon medium.

D. Proton charge radius

We now turn to the proton charge radius. For comparison, we calculate both the baryon charge radius and the electric charge radius, following Ref. [5], but generalized to include the BPS-Skyrme term, see Eq. (40). The baryon charge radius, defined in Eq. (41), is shown in Fig. 11 and the electric charge radius is shown in Fig. 12.

The model generally overestimates the proton charge radius. If we begin with Fig. 11, we can see that the loosely bound potential—although lowering the binding

energy—increases the baryon charge radius. This can readily be understood as follows. The loosely bound potential, like the mass term, decreases the size of the 4-Skyrmion. However, since it is calibrated against the physical size of helium-4, this implies a prolongation of the length scales. Because the 1-Skyrmion is more compact, it does not shrink as much as the 4-Skyrmion in the presence of the loosely bound potential, and with the prolonged length scales, its size increases. This yields a larger proton radius for larger values of the coefficient of the loosely bound potential, m_2. Interestingly, and counterintuitively, an increase of the pion mass for fixed larger m_2, see Fig. 11, yields a *smaller* baryon charge radius. The effect is however relatively small compared to that of changing m_2.

Since the proton is an electrically charged object, it has a well-defined electric charge radius, which is experimentally much more easily accessible than the baryon charge radius. From Eq. (40), however, we can see that half of the electric charge is given by the baryon charge, so the influence of the latter is 50%. Nevertheless, we can see from Fig. 12 that the electric charge radius has quite a different behavior in the parameter space than the baryon charge radius.

We can see that the electric charge radius is generally quite a bit larger than the baryon charge radius. This is physically reasonable. In general, it is seen that the BPS-Skyrme term helps decreasing the electric charge radius, but not nearly enough to reach the experimentally measured value. We can also see that a larger value of the pion mass again helps decreasing the radius.
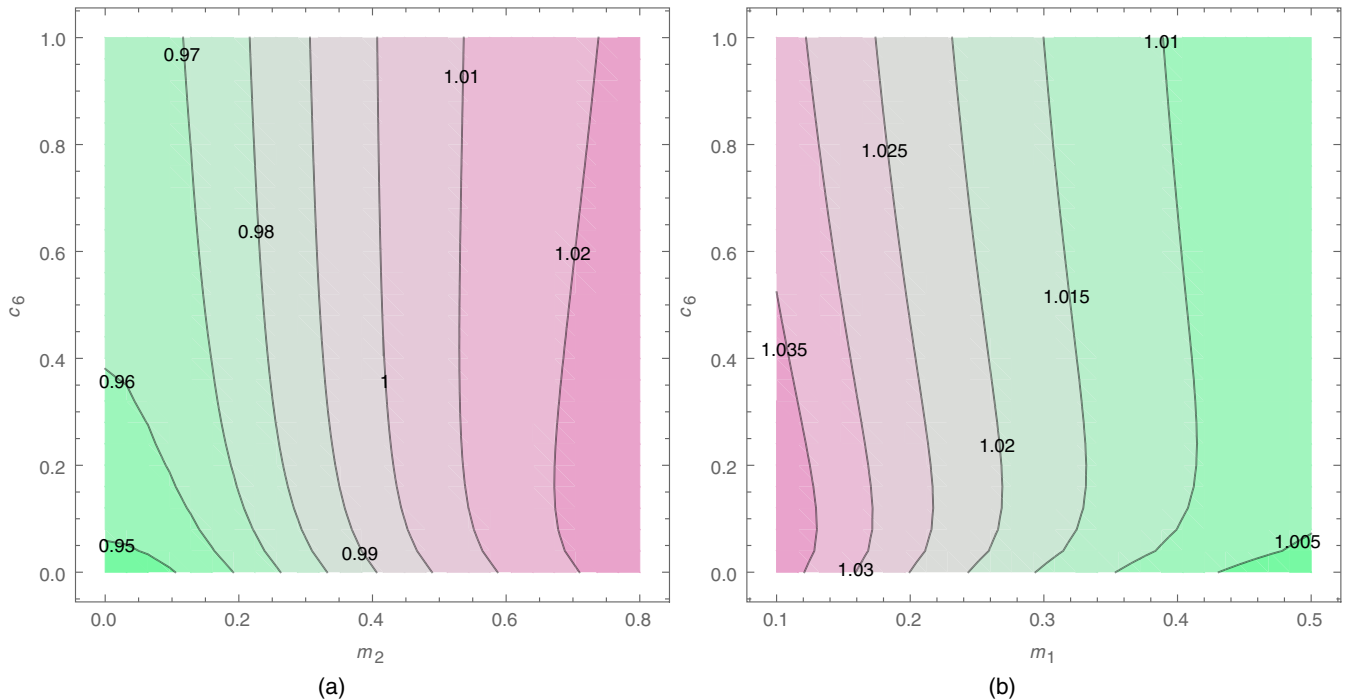

FIG. 11.   Baryon charge radius of the proton, r_1 [fm], in (a) the (m_2, c_6) plane for $m_1 = 0.25$ and (b) the (m_1, c_6) plane for $m_2 = 0.7$.
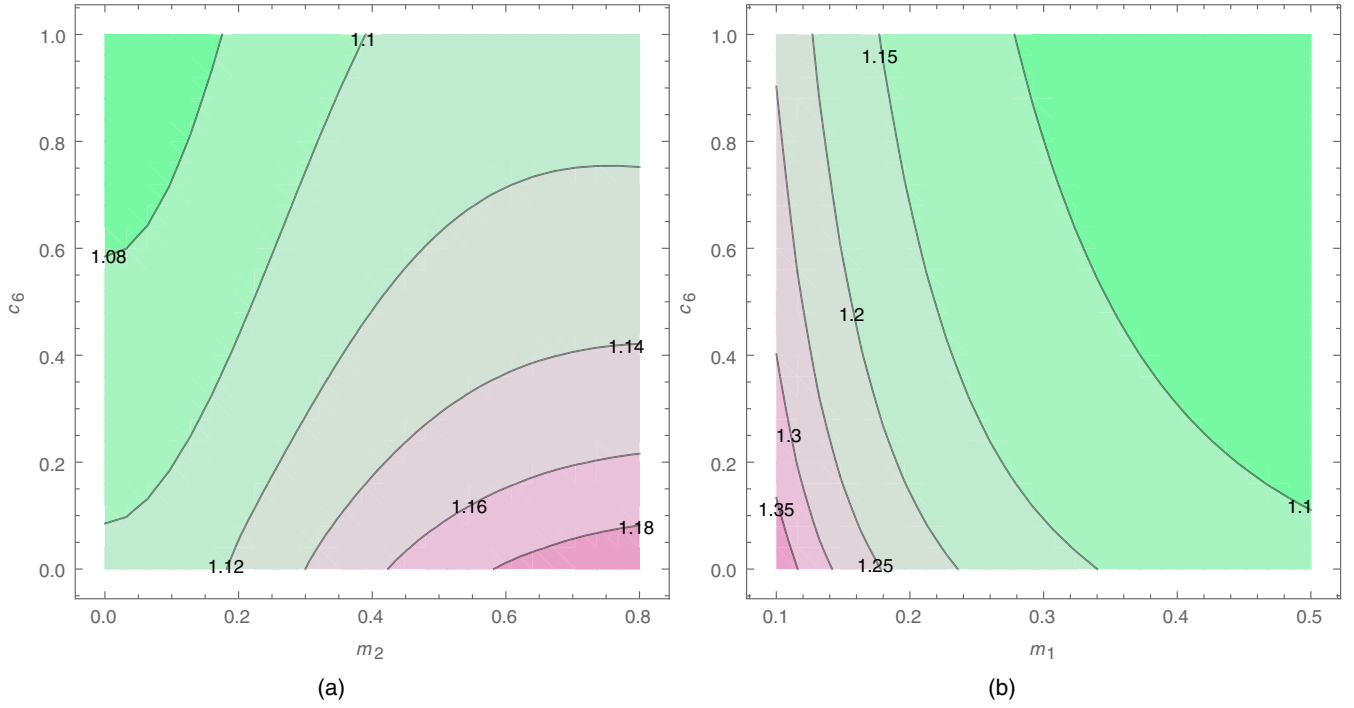
FIG. 12.   Electric charge radius of the proton, $r_{E,1}$ [fm], in (a) the (m_2, c_6) plane for $m_1 = 0.25$ and (b) the (m_1, c_6) plane for $m_2 = 0.7$.
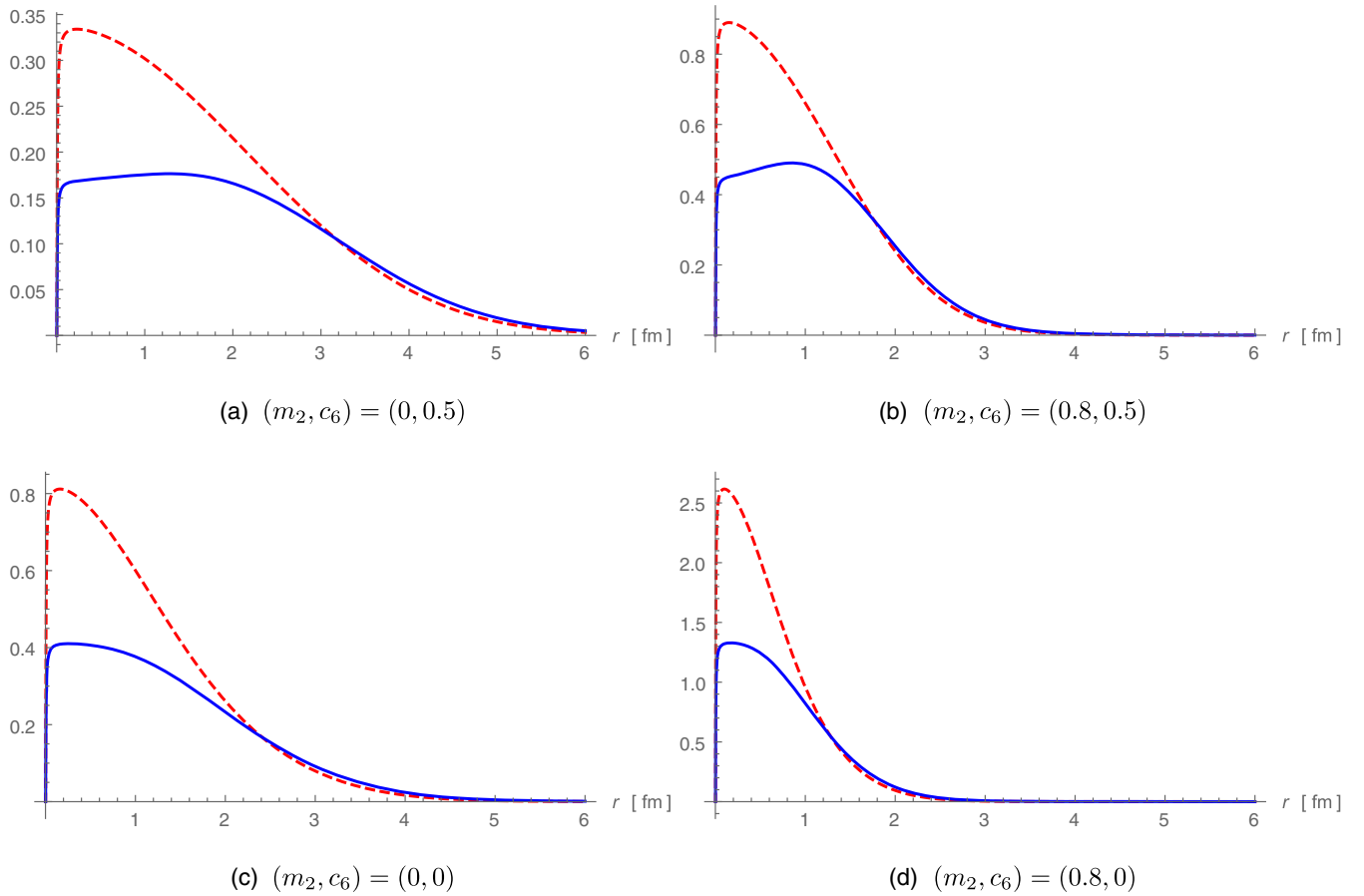

(a) $(m_2, c_6) = (0, 0.5)$

(b) $(m_2, c_6) = (0.8, 0.5)$

(c) $(m_2, c_6) = (0, 0)$

(d) $(m_2, c_6) = (0.8, 0)$

FIG. 13.   Baryon and electric charge densities, $\frac{1}{2\pi^2}\mathcal{B}^0$ as red dashed lines and ρ_E as blue solid lines, in various points of the parameter space: $(m_2, c_6) = (0.5, 0), (0.5, 0.8), (0, 0), (0, 0.8)$.
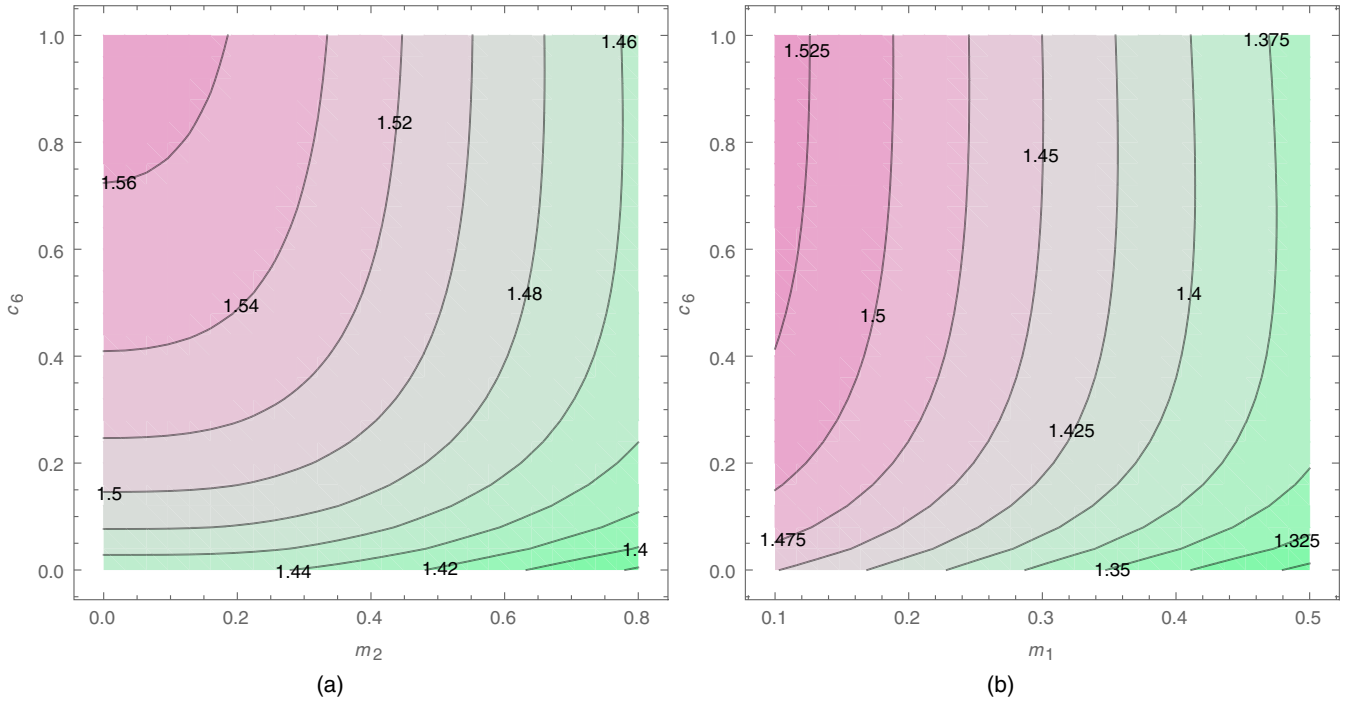
FIG. 14. Axial coupling, g_A, in (a) the (m_2, c_6) plane for $m_1 = 0.25$ and (b) the (m_1, c_6) plane for $m_2 = 0.7$.

As an example, we illustrate the baryon and electric charge densities in four points of the parameter space in Fig. 13.

E. Axial coupling

The final observable that we will present in this paper is the axial coupling, following Ref. [5], but again with the inclusion of the contribution from the BPS-Skyrme term, see Eq. (46). The result of the axial coupling in the chosen parameter space is shown in Fig. 14.

Although the original calculation in Ref. [5] yielded a value of g_A almost half the size of the experimentally measured value, our model overestimates this observable. This can be traced back to the value of the Skyrme-term coefficient, e, which is much smaller in our model when calibrated against the mass and size of helium-4. Although we overestimate the value of the axial coupling, we can see that if we were to increase m_2 beyond the chosen parameter space for large values of c_6, and possibly also increase the pion mass, the value could conceivably decrease to the right orders of magnitude of the experimentally measured value of about 1.27 [42]. That part of parameter space is, however, inaccessible in this paper because we cannot know if the cubic symmetry of the 4-Skyrmion is retained there or not. That requires the full PDE calculations and will be interesting land to cover in the near future.

F. Summary of the results

The loosely bound potential decreases the classical and total binding energies [30,31], and in this paper, we have

shown that the BPS-Skyrme term with an order-one coefficient can help decreasing it further. In particular, for $m_2 = 0.8$: increasing c_6 to $c_6 = 1$, decreases the binding energy by 0.9% (after taking the calibration into account), and it worsens the values of the nucleon mass, axial charge and spin contribution to the nucleon; it improves the value of the proton charge radius; has no effect on the Δ mass and pion decay constant; and it overshoots the value of the pion mass. The tendencies seen in our results in this section, indicate that enlarging the parameter space using full PDE calculations, one may find solutions with lower and more realistic binding energies than found in this paper.

V. DISCUSSION

In this paper, we have studied the most accessible part of the parameter space of the loosely bound Skyrme model with the BPS-Skyrme term and the second-order potential providing the lowest binding energies. For the first time, we have used the rational map approximation for the Skyrme model quite far outside of its common range; that is, we have turned on both the loosely bound potential and the BPS-Skyrme term.[4] Interestingly, the same function of the rational map applies to the BPS-Skyrme term as appeared already in the normal Skyrme term. For the loosely bound potential, we could compare our results to those of

---

[4]The rational map is often used in the (pure) BPS-Skyrme model [18,19], where it is not an approximation due to volume-preserving diffeomorphism invariance.

Ref. [31] and calculate the systematic error by using the rational map approximation: about 1.5%–2.5%, with an approximate linear increase as function of the coefficient of the loosely bound potential, m_2. We have found the classical binding energy as low as 1.8% and total binding energy down to about 5.3%, in the covered part of parameter space. With the results of Ref. [31] in mind, we expect that in the part of parameter space where the pion mass is large, the coefficient of the loosely bound potential is allowed to be larger than covered here and then turning on a sizable BPS-Skyrme term will result in even lower binding energies.

Another result that we have calculated in this paper is the contribution from the BPS-Skyrme term to the axial coupling. It generally increases the value of the coupling, which is a wanted feature in light of the original results [5]; however, with our calibration the coupling turns out to be slightly too large compared with its experimental value. Fortunately, the tendency of the results in this paper points in the direction that the region of parameter space where we may lower the binding energy further than what we have covered in this paper may lead to a lower and perhaps quite reasonable value of the axial coupling.

If we pick the vanilla point in our covered parameter space—based entirely on the binding energy—we get a total binding energy of 5.3%, the pion decay constant at 71 MeV, $e \sim 4.5$, the nucleon mass at 960 MeV, the mass of the Delta resonance at 1095 MeV, the pion mass at 75 MeV, the proton charge radius at 1.25 fm, and finally, the axial coupling at 1.53. A comparably good point in parameter space gives us instead, a total binding energy of 5.5%, the pion decay constant at 65 MeV, $e \sim 4.6$, the nucleon mass at 960 MeV, the mass of the delta at 1100 MeV, the pion mass at 150 MeV, the proton charge radius at 1.15 fm, and finally, the axial coupling at 1.46.

The first thing that can be done from now is to explore the parameter space of the loosely bound Skyrme model with the BPS-Skyrme term turned on using full PDE calculations. This will first of all confirm our results here (we expect 1%–2% error and perhaps less after correcting for the systematic error at the $c_6 = 0$ slice of parameter space), but it will also allow one to go farther into unexplored regions of parameter space, which are expected to contain solutions with even lower binding energies than found in this paper. There are two directions to explore. The first is towards the near-BPS regime of the BPS-Skyrme model which in our language means very large

values of c_6 and m_2. The problem with this approach is the technically difficult numerical calculations that need to be tackled. The other direction to search in, is to take a large pion mass; crank up m_2 to the boundary of where the cubic symmetry of the 4-Skyrmion is lost and then increase c_6 (the BPS-Skyrme term) and again increase m_2 as much as possible. Continue this loop until the binding energy is of the right order of magnitude (or until a technical problem occurs).

Another interesting future direction would be to consider the derivation of the BPS-Skyrme term in the framework of partially bosonized QCD at large N_c, along the lines of Ref. [32].

Let us mention an obstacle that we have not mentioned so far. We are pursuing the lowest possible binding energies in a generalization of the Skyrme model in order to match experimental data. However, even if we can reduce the classical binding energy arbitrarily, say down to ε, then the tendency is that the method of adding the quantized spin-isospin contribution to the classical mass by itself yields about 2%–3% binding energy. Thus to reach agreement with experiments, we need a classical binding energy of about $-(1\%–2\%)$, which means that the classical solutions are unbound and thus impossible. It is plausible that vibrational modes could play a role in this problem (like for ^{7}Li and ^{16}O in Refs. [43–45]), so that the 4-Skyrmion would receive a nonrotational quantum contribution and thus lower its binding energy. This issue of the large size of the spin-isospin contribution to the 1-Skyrmion has been addressed recently in Ref. [46], where it was suggested by an indirect argument of relating the spin contribution to the nucleon mass and the moment of inertia of the nucleon, that the spin contribution should actually be more than twice as large as the standard Skyrme model (direct) argument suggests. The spin contribution to the mass of the nucleon needed should, by comparing the nucleon to helium-4, be as low as 7.2 MeV. However, by the indirect argument of Ref. [46], it could be as large as 16 MeV, reducing a lot of tension in the Skyrme model. For consistency, however, this requires *some* quantum contribution to the 4-Skyrmion.

[1] T. H. R. Skyrme, A unified field theory of mesons and baryons, Nucl. Phys. **31**, 556 (1962).

[2] T. H. R. Skyrme, A nonlinear field theory, Proc. R. Soc. A **260**, 127 (1961).

[3] E. Witten, Global aspects of current algebra, Nucl. Phys. **B223**, 422 (1983).

[4] E. Witten, Current algebra, baryons, and quark confinement, Nucl. Phys. **B223**, 433 (1983).

[5] G. S. Adkins, C. R. Nappi, and E. Witten, Static properties of nucleons in the Skyrme model, Nucl. Phys. **B228**, 552 (1983).

[6] I. Zahed and G. E. Brown, The Skyrme model, Phys. Rep. **142**, 1 (1986).

[7] R. A. Battye and P. M. Sutcliffe, Symmetric Skyrmions, Phys. Rev. Lett. **79**, 363 (1997).

[8] C. J. Houghton, N. S. Manton, and P. M. Sutcliffe, Rational maps, monopoles and Skyrmions, Nucl. Phys. **B510**, 507 (1998).

[9] R. A. Battye and P. M. Sutcliffe, Skyrmions, fullerenes and rational maps, Rev. Math. Phys. **14**, 29 (2002).

[10] R. Battye and P. Sutcliffe, Skyrmions and the pion mass, Nucl. Phys. **B705**, 384 (2005).

[11] R. Battye and P. Sutcliffe, Skyrmions with massive pions, Phys. Rev. C **73**, 055205 (2006).

[12] C. Houghton and S. Magee, The effect of pion mass on skyrme configurations, Europhys. Lett. **77**, 11001 (2007).

[13] R. Battye, N. S. Manton, and P. Sutcliffe, Skyrmions and the alpha-particle model of nuclei, Proc. R. Soc. A **463**, 261 (2007).

[14] M. Freer, The clustered nucleus–cluster structures in stable and unstable nuclei, Rep. Prog. Phys. **70**, 2149 (2007).

[15] P. H. C. Lau and N. S. Manton, States of Carbon-12 in the Skyrme Model, Phys. Rev. Lett. **113**, 232503 (2014).

[16] P. Sutcliffe, Skyrmions, instantons and holography, J. High Energy Phys. 08 (2010) 019.

[17] P. Sutcliffe, Skyrmions in a truncated BPS theory, J. High Energy Phys. 04 (2011) 045.

[18] C. Adam, J. Sanchez-Guillen, and A. Wereszczynski, A Skyrme-type proposal for baryonic matter, Phys. Lett. B **691**, 105 (2010).

[19] C. Adam, J. Sanchez-Guillen, and A. Wereszczynski, A BPS Skyrme model and baryons at large N_c, Phys. Rev. D **82**, 085015 (2010).

[20] C. Adam, C. Naya, J. Sanchez-Guillen, R. Vazquez, and A. Wereszczynski, The Skyrme model in the BPS limit, arXiv:1511.05160., *The Multifaceted Skyrmion, 2nd Edition* edited by M. Rho and I. Zahed (World Scientific, Singapore, 2015).

[21] L. D. Faddeev, Some comments on the many dimensional solitons, Lett. Math. Phys. **1**, 289 (1976).

[22] N. S. Manton and P. J. Ruback, Skyrmions in flat space and curved space, Phys. Lett. B **181**, 137 (1986).

[23] C. Adam, C. Naya, J. Sanchez-Guillen, J. M. Speight, and A. Wereszczynski, Thermodynamics of the BPS Skyrme model, Phys. Rev. D **90**, 045003 (2014).

[24] C. Adam, C. Naya, J. Sanchez-Guillen, R. Vazquez, and A. Wereszczynski, BPS Skyrmions as neutron stars, Phys. Lett. B **742**, 136 (2015).

[25] C. Adam, C. Naya, J. Sanchez-Guillen, R. Vazquez, and A. Wereszczynski, Neutron stars in the Bogomol'nyi-Prasad-Sommerfield Skyrme model: Mean-field limit versus full field theory, Phys. Rev. C **92**, 025802 (2015).

[26] C. Adam, M. Haberichter, and A. Wereszczynski, Skyrme models and nuclear matter equation of state, Phys. Rev. C **92**, 055807 (2015).

[27] M. Gillard, D. Harland, and M. Speight, Skyrmions with low binding energies, Nucl. Phys. **B895**, 272 (2015).

[28] J. M. Speight, Near BPS skyrmions and restricted harmonic maps, J. Geom. Phys. **92**, 30 (2015).

[29] D. Harland, Topological energy bounds for the Skyrme and Faddeev models with massive pions, Phys. Lett. B **728**, 518 (2014).

[30] S. B. Gudnason, Loosening up the Skyrme model, Phys. Rev. D **93**, 065048 (2016).

[31] S. B. Gudnason and M. Nitta, Modifying the pion mass in the loosely bound Skyrme model, Phys. Rev. D **94**, 065018 (2016).

[32] A. Zaks, Derivation of the Skyrme-witten Lagrangian from QCD, Nucl. Phys. **B260**, 241 (1985).

[33] A. Ebrahim and M. Savci, Derivation of the Skyrme Lagrangian, Phys. Lett. B **171**, 429 (1986).

[34] T. Sakai and S. Sugimoto, Low energy hadron physics in holographic QCD, Prog. Theor. Phys. **113**, 843 (2005).

[35] G. S. Adkins and C. R. Nappi, Stabilization of chiral solitons via vector mesons, Phys. Lett. **137B**, 251 (1984).

[36] A. Jackson, A. D. Jackson, A. S. Goldhaber, G. E. Brown, and L. C. Castillejo, A modified skyrmion, Phys. Lett. **154B**, 101 (1985).

[37] G. H. Derrick, Comments on nonlinear wave equations as models for elementary particles, J. Math. Phys. (N.Y.) **5**, 1252 (1964).

[38] N. S. Manton and P. Sutcliffe, *Topological Solitons* (Cambridge University Press, Cambridge, England, 2004).

[39] V. B. Kopeliovich, MultiSkyrmions and baryonic bags, J. Phys. G **28**, 103 (2002).

[40] S. Dube and L. Marleau, Phenomenological implications of a generalized Skyrme model, Phys. Rev. D **41**, 1606 (1990).

[41] L. Marleau, Modifying the Skyrme model: Pion mass and higher derivatives, Phys. Rev. D **43**, 885 (1991).

[42] K. A. Olive *et al.* (Particle Data Group Collaboration), Review of Particle Physics, Chin. Phys. C **38**, 090001 (2014).

[43] C. J. Halcrow, Vibrational quantisation of the B = 7 Skyrmion, Nucl. Phys. **B904**, 106 (2016).

[44] C. J. Halcrow, C. King, and N. S. Manton, A dynamical α-cluster model of ^{16}O, arXiv:1608.05048.

[45] M. C. Davies and L. Marleau, Skyrmion vibrational energies together with a generalized mass term, Phys. Rev. D **79**, 074003 (2009).

[46] C. Adam, J. Sanchez-Guillen, and A. Wereszczynski, On the spin excitation energy of the nucleon in the Skyrme model, Int. J. Mod. Phys. E, doi: 10.1142/S021830131650097X (2016).